

# Coded Power Transfer

Sudip K. Mazumder, *Fellow, IEEE*

**Abstract**—This manuscript captures in brief a core innovation in the two patented technologies. The underlying focus of the two technologies is to demonstrate how discrete energy transfer can be achieved that leads enhanced power-conversion efficiency in one case and a mechanism for packetized energy transfer that can enable co-transfer of information and energy.

**Index Terms**—Energy, discrete, coding, converter, packet, modulation

## I. INTRODUCTION

POWER-electronic systems including but not limited to solid-state transformers, indirect matrix converters, galvanically-isolated electric-vehicle chargers, and high-frequency-link (HFL) converters often have multiple stages of power conversion. Usually, switching of the devices of each of these power-conversion stages follow some modulation principle(s) that yields desired goal(s). Often, the information generated in the pulsating intermediate power signals are lost due to intermediate filtering (e.g., dc link) that lands up requiring additional switching or forced commutation. For one such HFL power-conversion system, a novel technology, referred to as hybrid modulation [1]-[3], was captured, which provides a unique mechanism of utilizing the “coded” information in the switching power signal due to modulated switching of the power semiconductor devices thereby reducing switching losses and eliminating the need for dc link capacitors and yielding reduced form factor. This is briefly illustrated in Section II.

While the hybrid modulation enables the coded power transfer in a multi-stage but typically single overall power-conversion system, another approach, outlined in Section III, relates to transfer of discretized energy transfer among distributed power converters [4][5]. Basically, in an embodiment, each power converter generates energy packets that are co-transferred with information in a mutually exclusive sequential manner. This is fundamentally different from relatively recent approaches where the same converter is used for energy and data transfer by leveraging the modulation of the converter [6]. The proposed approach achieves high baud rate since the data transfer is not at high voltage and hence not limited by the capacitance of the power semiconductor device. Because the data and the energy packets are mutually exclusive in one embodiment of the proposed approach, possibility of interference is essentially eliminated. By generating such discretized energy packets transmitted at high frequency (with appropriate coding) for an energy receiver or a set of energy receivers, applications such as distributed energy storage can reduce size and weight of systems or overall efficiency of a network could be improved.

## II. HYBRID MODULATION OF HFL INVERTER

Fig. 1 [2] shows capacitorless pulsating-dc-link HFL inverter. In this topology, the dc input is first converted into a HF AC, then rectified, and then converted to a sinusoidal PWM signal for three-phase output. What is novel in this approach is that the information that is “coded” in the first stage (i.e., HF inverter) of the overall HFL inverter is never lost unlike a conventional fixed-dc-link or unfolding-link inverter (which requires HF switching of the final stage). Instead, the final stage of the overall HFL inverter simply uses the coded pulse sequence available at the pulsating dc link to generate the needed sinusoidally-modulated switching signals simply by switching (for any 60-degree sector) only one of the legs at HF while the other two legs do not change their switching states. This reduces the switching loss of the final stage by 66% without requiring any complex soft switching and any large dc-link capacitor. This is illustrated in Fig. 2 [2].

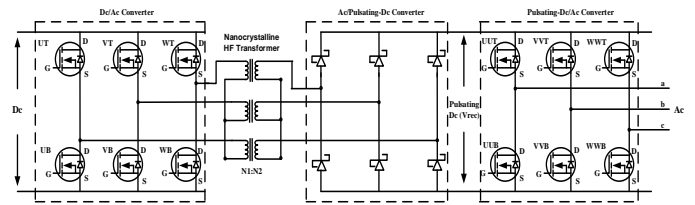


Fig. 1. Topology of a capacitorless pulsating-dc-link HFL inverter.

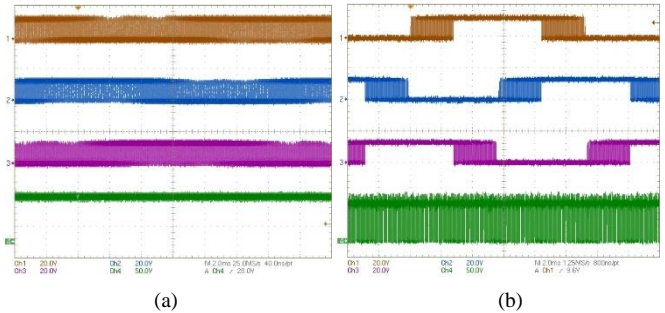


Fig. 2. Experimental illustration: (a) PWM signals of a conventional fixed-dc-link inverter that requires HF switching of all legs of the output stage since the coded information is lost in the dc link; (b) hybrid modulation, instead, requires switching of only 1 leg at HF since the pulsating-dc link retains the sinusoidally-modulated information coded by the first stage. It is referred to as hybrid modulation because (and unlike conventional) discontinuous modulation while 1 output stage operates at HF, the other 2 stages at low frequency.

Additional work has shown that if the coding of the front-stage HF inverter is so done such that it not only generates sinusoidally-modulated power signals, but also leverages pulse placement, then, additional improvement in input current THD can be achieved [7] due to this two-dimensional modulation scheme that generates a different coded power-signal pattern. Yet another work has demonstrated if the front-end inverter has a V6 topology (instead of the V3 topology or one with 3 bridges as shown in Fig. 1), then, even the remaining 33% switching

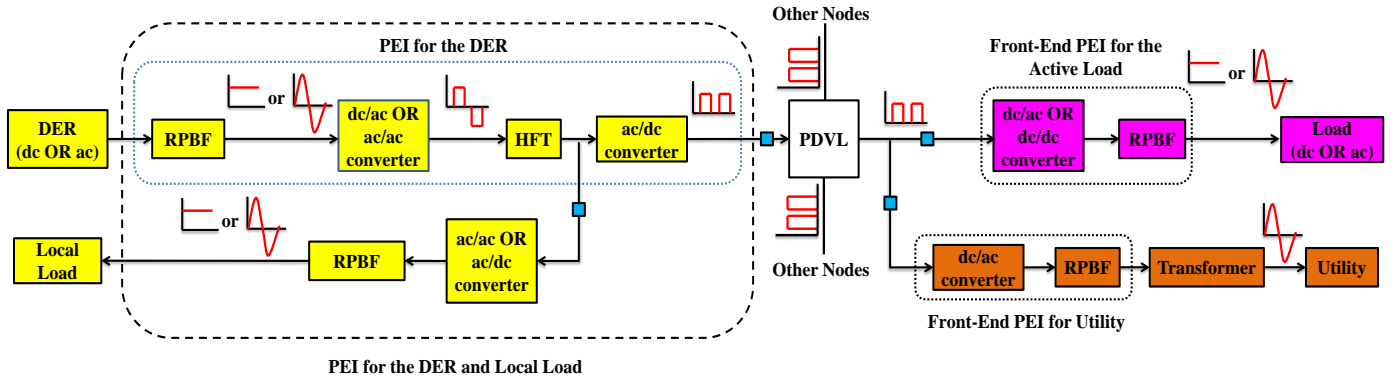


Fig. 3: An illustrative power-electronic-interface (PEI) mechanism for creating a pulsating-dc-voltage-link (PDVL) leading to an illustrative SIMO realization. The PDVL is illustrated in Fig. 4. Also illustrated are the PEIs for the distributed energy resource (DER) and the local load, distributed load, and the utility grid. Voltage signals at different stages are shown in red. It is noted that, power flow can be bi-directional depending on a load or a DER even though not explicitly shown. RPF represent ripple power balancing filter while HFT represents high frequency transformer which may be necessary is isolation is needed.

loss of the final stage of the HFL inverter can also be eliminated [3]. This is achieved by generating two time-staggered pulse sequence at the output of the front-end HF inverter, which ensures the availability of the complete coded information at the pulsating-dc link and eliminates the need for any HF switching for the final HFL inverter stage thereby yielding 100% switching loss elimination.

Since its inception, the hybrid-modulation based inverter has found application in solar- and fuel-cell inverters, solid-state transformer, and electric-vehicle fast battery charger.

### III. BOOLEAN ENERGY GRID

The question now arises, what happens if the pulsating-dc link, outlined in Section II, is not terminated in only one final stage converter? Can it be fed to multiple such output stages with some front-end routing if necessary. The answer to that is a yes for such a single-input-single-output (SISO) or single-input-multiple-output (SIMO) realizations, as illustrated in Fig. 3. In fact, one can generalize the idea to even a MISO or MIMO realization [4][5].

The advantage that was realized for a single pulsating-dc-link HFL inverter outlined in Section II, can now be extended to an entire network of power-electronic systems. Unlike the conventional dc and 60/50 Hz ac energy transfer, with continuous energy transfer, in this new approach discretized energy is transferred from single or plural energy source(s), like information data packets in communication systems, which can be routed to single or multiple energy sink(s) or loads. An illustrative advantage embodiment is that, since the discretized energy is sent in fast and but smaller energy packets, the distributed energy storage requirements can be reduced significantly. Further, the energy packets can be coded in such a way (following Section II) such that downstream switching requirements could be reduced thereby yielding higher efficiency. Further, since the energy packets are discretized, they themselves can be coded (e.g., placing the pulses at different temporal location in a periodic cycle) to convey information for downstream converters yielding additional advantages including but not limited to security.

Yet another major advantage of the discretized energy transfer implies that when energy is not being transferred, data can be transferred rapidly over the same channel since there is no high-voltage signal at that instant on the PDVL shown in Fig. 3. This implies that one can now realize a Boolean energy grid where discretized energy and data can be transmitted mutually exclusively, as illustrated in Fig. 4.

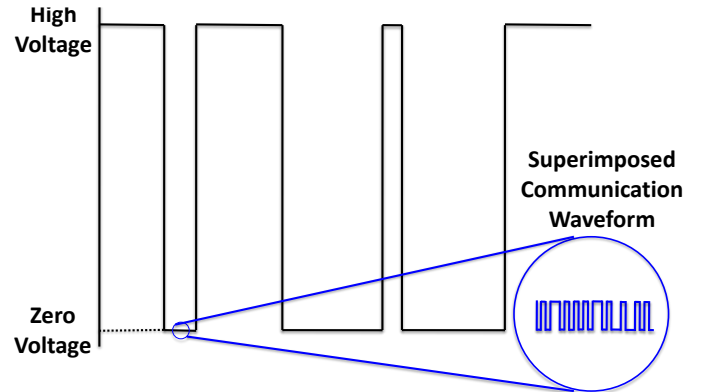


Fig. 4. Illustration of the PDVL in Fig. 3 supporting discrete energy and data for a Boolean realization.

The illustrative synthesis of the mutually-exclusive realization is captured in Fig. 5. It shows how an  $n$ th source-side power node (PNnS) transfers energy to a  $n$ th load-side power node (PNnL) over a common HF channel if only the routing switches  $S_{nPS}$  and  $S_{nPL}$  are simultaneously activated. During this time, the data network is inactive. This synchronization of  $S_{nPS}$  and  $S_{nPL}$  is achieved by pre-transferring information over the data network from the source-side data-network node DNnS to the load-side data-network node DNnL over the common channel. During this time, only  $S_{nDS}$  and  $S_{nDL}$  are simultaneously activated and  $S_{nPS}$  and  $S_{nPL}$  are turned off. It is noted that, the information transferred over the data network is not limited to synchronization information. The mutual exclusivity of energy and information ensures limited or no coupling as demonstrated in [5].

Since its inception, this concept has been explored for solid-state lighting, distributed energy storage, and Boolean microgrid.

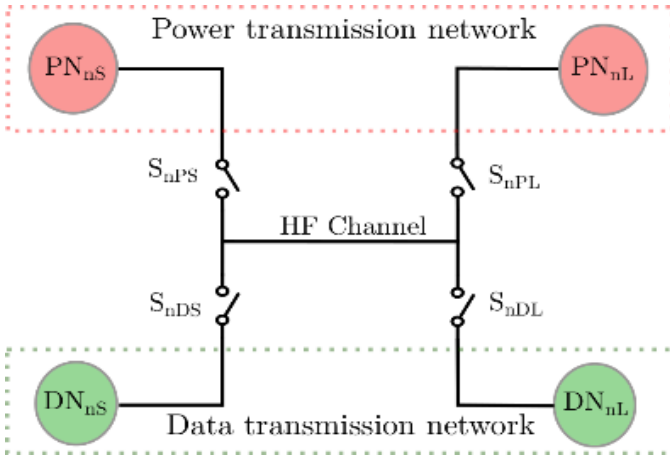
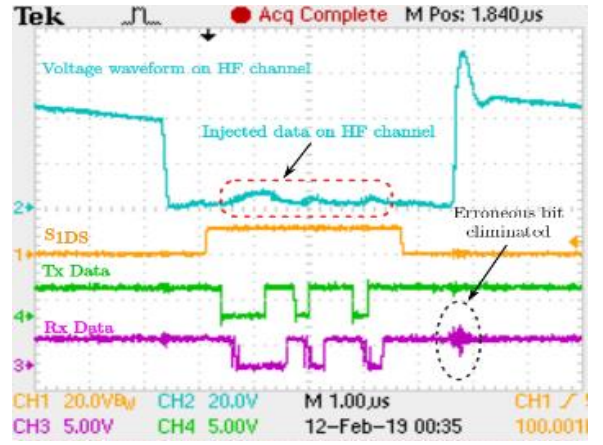
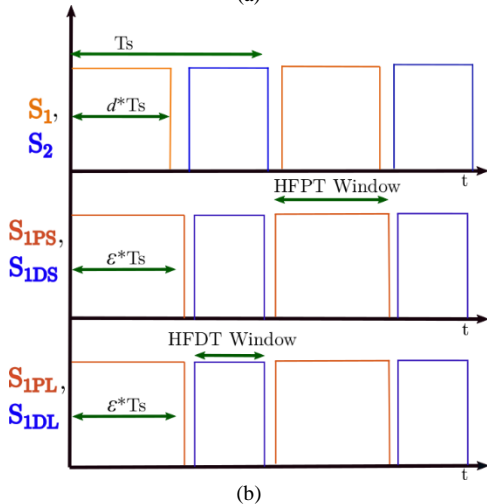
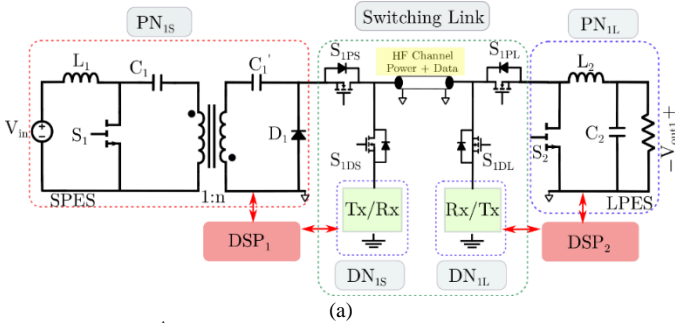


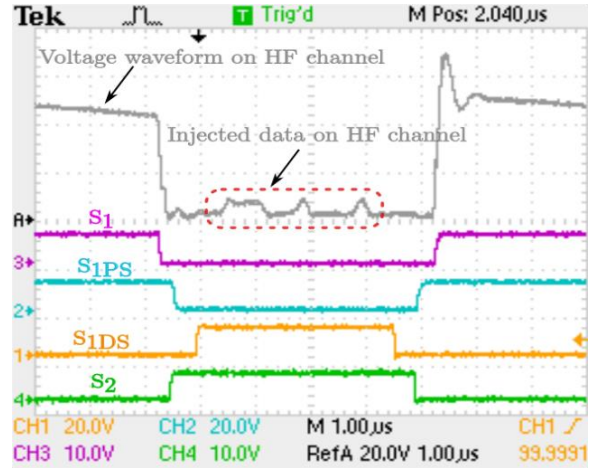
Fig. 5. An illustrative realization of the mutually exclusive power and data transfer.

### A) SISO Realization

Fig. 6 captures an experimental snapshot that validates the operation of this Boolean energy and information transfer mechanism. The schematic of the single-input-single-output (SISO) HF distributed power system (HFDPS) is captured in Fig. 6a along with timing diagram in Fig. 6b (illustrating HF power and data transfer (HFPT/HFDT) windows over a time horizon  $T_s$ ) and the details are provided in [9]. In Fig. 6c, to the left and right of the waveform, power is being transferred as indicated by higher voltage on the HF channel and S1DS toggling to a low state. Once S1DS toggles high, data transfer over the same HF channel is initiated while power transfer is disabled.



(c)



(d)

Fig. 6. (a) A SISO HFDPS for implementing Boolean power and data transfer. Operational details are provided in [9]. (b) Timing diagram of key switches. (c), (d) Experimental result showing the efficacy of the Boolean power and data transfer.

### B) SIMO Realization

A SIMO HFDPS realization is illustrated in Fig. 7.  $PN_{1S}$  serves as the source power node while  $PN_{1L}$  and  $PN_{2L}$  serve as the two load nodes. Power nodes  $PN_{1S}$ ,  $PN_{1L}$ , and  $PN_{2L}$  and data nodes  $DN_{1S}$ ,  $DN_{1L}$  and  $DN_{2L}$  are connected to the HF channel using transfer switches  $S_{1PS}$ ,  $S_{1PL}$ , and  $S_{2PL}$  and data switches  $S_{1DS}$ ,  $S_{1DL}$ , and  $S_{2DL}$ , respectively.

Consistent with a SISO HFDPS, in a SIMO HFDPS following sequential co-transfer scheme, transfer and data switches are operated in a mutually exclusive manner. Each combination of a power node and its corresponding data node is managed using a separate digital controller  $DSP_1$  or  $DSP_2$ .

$DSP_1$  coordinates locally with  $PN_{1S}$  for gating signals and feedback signals,  $DN_{1S}$  regarding data communication and mode selection and switching-link regarding sequential power and data co-transmission. Similar roles are performed by  $DSP_2$  and  $DSP_3$  for power node  $PN_{1L}$  and  $PN_{2L}$ , data node  $DN_{1L}$  and  $DN_{2L}$  and the switching-link. When working together, coded data is exchanged between the data nodes, and power packets generated by  $PN_{1S}$  are routed to  $PN_{1L}$  and  $PN_{2L}$  following time division multiplexing (TDM).

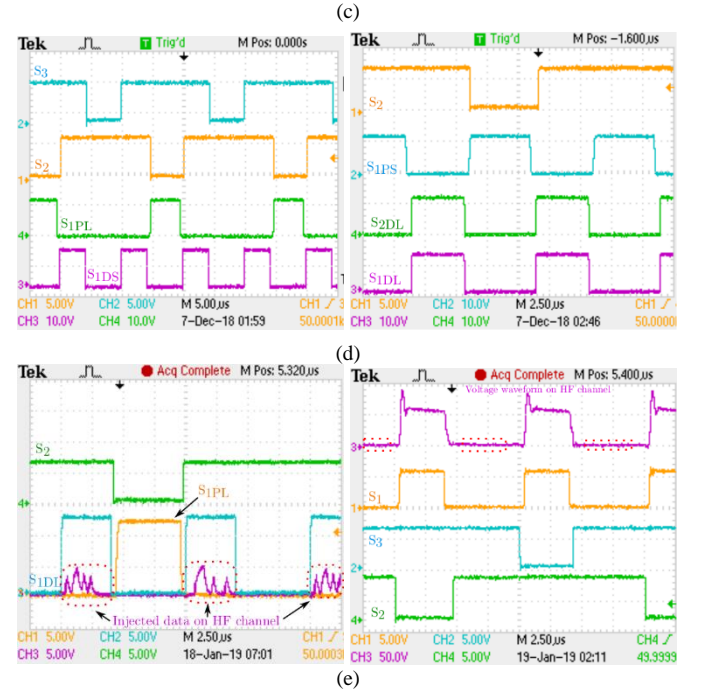
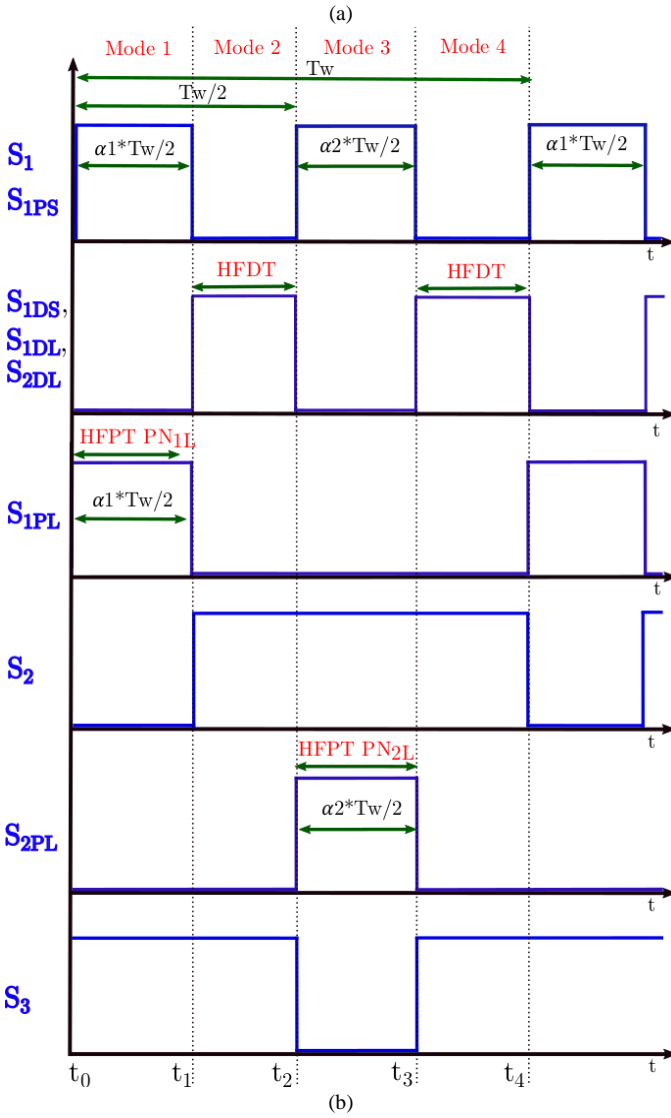
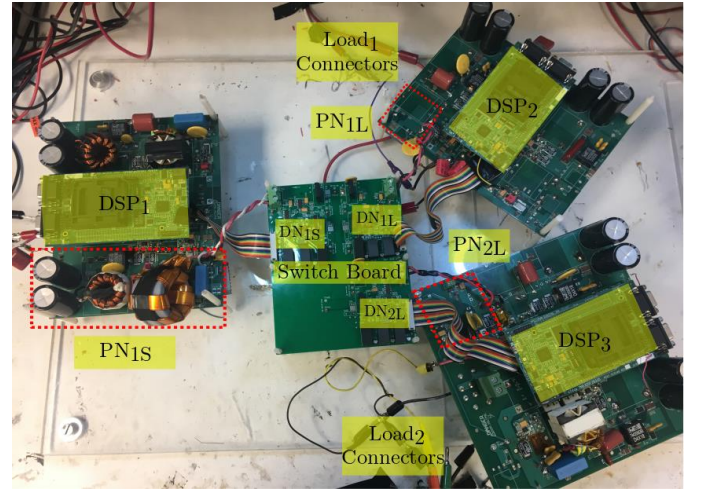
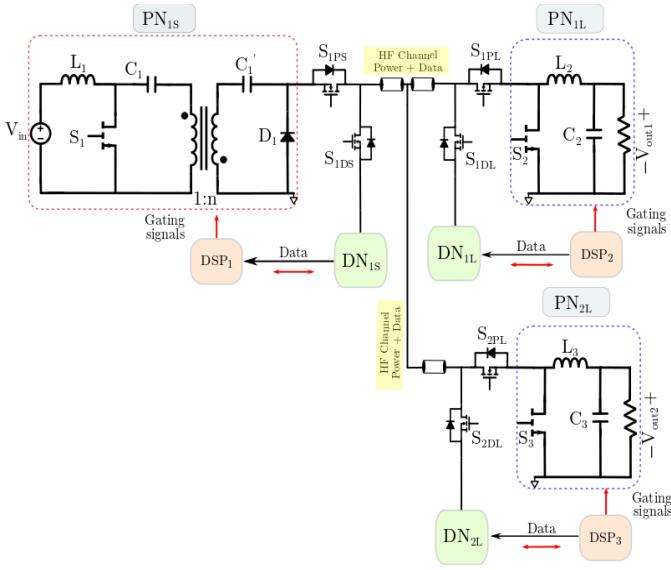


Fig. 7. (a) A SIMO HFDPS for implementing Boolean power and data transfer and the (b) associated timing diagram. (c) An experimental SIMO HFDPS setup and (d) associated gating signals, and (e) experimental waveforms showing the transfer of HF data signals over the HF channel, along with the gating signals for  $S_{1DL}$ ,  $S_{1PL}$ , and  $S_2$  at  $PN_{1S}$ , and experimental waveform showing sequential co-transfer of HF power and data over the HF channel in a SIMO HFDPS along with the gating signals for  $S_1$ ,  $S_3$ , and  $S_2$ .

Timing diagram of the SIMO HFDPS is shown in Fig. 7b. In it,  $T_w$  represents the time duration of a TDM frame required for routing HF power and data packets in the designed SIMO HFDPS. Since in the designed SIMO HFDPS, HF power packet needs to be routed to the two LPES, the TDM frame is subdivided in two equal time slots each with a duration of  $T_w/2$ . During the time interval  $t_0 - t_1$ , the HF power packet is routed from  $PN_{1S}$  to  $PN_{1L}$  and during the time interval  $t_2 - t_3$ , HF power packet is routed from  $PN_{1S}$  to  $PN_{2L}$ , these durations are marked as HFPT  $PN_{1L}$  and HFPT  $PN_{2L}$ , respectively. The HF channel is available for data transferred during the time intervals  $t_1 - t_2$  and  $t_3 - t_4$ , these durations are marked as

HFDT. Additionally,  $\alpha_1$  and  $\alpha_2$  are the time-allocation values requested by the load and determine the size of the HF power packet generated by the power transmitter node. Since,  $T_W$  is the total time required for completing a full HF power and data transfer cycle for the designed SIMO HFDPS, it also represents the switching cycle time for all the power nodes in which they need to achieve their inductor charge balance and capacitor voltage balance for ensuring a stable steady state operation.

An illustrative experimental setup for the SIMO realization is captured in Fig. 7c along with experimental results in Figs. 7d and 7e. These results are obtained with each load node terminating in separate passive load. In contrast, Fig. 8 shows the output waveform when the two outputs in Fig. 7a are connected in a differential-mode configuration with an ac passive load and each load node receiving sinusoidally coded energy packets yielding a familiar sinusoidal (inverter) ac output voltage and current [13] with the exception that routing eliminates about 25% of the power-stage hardware in [13].

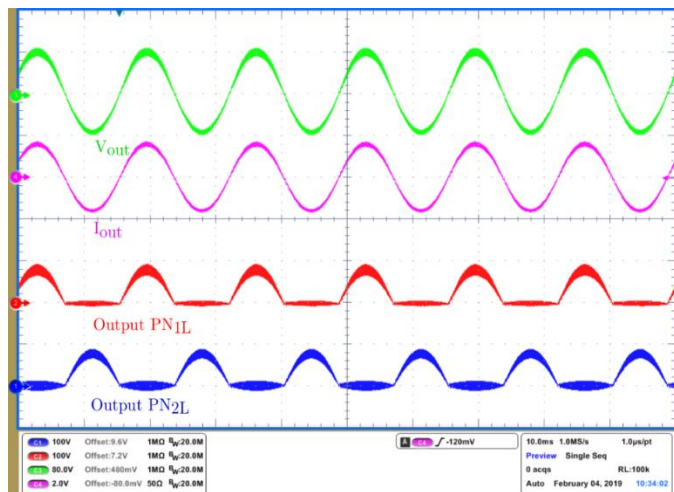


Fig. 8. Results for a SIMO HFDPS with the two load nodes connected in a differential-mode configuration.

#### IV. CONCLUSIONS

In this brief letter, the utility of coding energy transfer, if done appropriately, has been illustrated using some novel innovations. Essentially, the technologies outlined have the potential to enable controlled intermediate digitized/discretized energy transfer and go beyond continuous power transfer thereby yielding advantages including but not limited to energy transfer efficiency, packetized energy controllability to name a few. Extending the concept from SISO to SIMO/MIMO will require further work not limited to stability, controllability, routing [8], and waveguide thereby providing further exciting possibilities. With regard to the first two issues, the fundamental work based on multi-scale modeling and stability of the author, as captured in [11][12] is an initial step in that direction that can assess stability and controllability in terms of the evolution of the switching states (i.e., switching sequences) of the power-conversion system and application load. Other small-signal approaches can also be found in the literature such as those captured in [13].

#### ACKNOWLEDGEMENT

This work was supported in part by the U.S. National Science Foundation under Award 0725887 entitled "Hybrid-Modulation based High-power High-frequency and Scalable SiC Polyphase Fuel-cell Inverter for Power Quality and Distributed Generation" in 2007 and under Award 1239118 entitled "CPS: Synergy: Collaborative Research: Boolean Microgrid" in 2012 received by Prof. Sudip K. Mazumder at the University of Illinois Chicago, USA.

#### REFERENCES

1. S.K. Mazumder and R. Huang, "Multiphase converter apparatus and method," USPTO Patent# 7,768,800 B2, awarded on Aug 3, 2010.
2. S. K. Mazumder, "Hybrid modulation scheme for a high-frequency ac-link inverter," in IEEE Transactions on Power Electronics, vol. 31, no. 1, pp. 861-870, Jan. 2016, doi: 10.1109/TPEL.2015.2411714.
3. A. Rahnamaee and S. K. Mazumder, "A soft-switched hybrid-modulation scheme for a capacitor-less three-phase pulsating-dc-link inverter," in IEEE Transactions on Power Electronics, vol. 29, no. 8, pp. 3893-3906, Aug. 2014, doi: 10.1109/TPEL.2013.2269141.
4. S. K. Mazumder and A. Gupta, "Systems and methods for co-transmission of discrete power and data," USPTO Patent # 11245437 B2, awarded on Feb 8, 2022.
5. A. Gupta and S. K. Mazumder, "Sequential co-transmission of high-frequency power and data signals," in IEEE Transactions on Industrial Informatics, vol. 14, no. 10, pp. 4440-4445, Oct. 2018, doi: 10.1109/TII.2018.2794373.
6. X. He, R. Wang, J. Wu, et al. "Nature of power electronics and integration of power conversion with communication for talkative power." Nat Commun 11, 2479 (2020). <https://doi.org/10.1038/s41467-020-16262-0>.
7. S. K. Mazumder and A. K. Rathore, "Impact of dc link pulse coding on the harmonic distortion of the high-frequency-link inverter," IECON 2010 - 36th Annual Conference on IEEE Industrial Electronics Society, 2010, pp. 499-504, doi: 10.1109/IECON.2010.5675202.
8. A. Gupta, N. Kumar and S. K. Mazumder, "Generalized input impedance modeling of TL-network-based HFDPS for validating frequency-dependent criteria for power-signal integrity," in IEEE Transactions on Industrial Electronics, vol. 65, no. 5, pp. 4114-4124, May 2018, doi: 10.1109/TIE.2017.2758739.
9. A. Gupta, "High frequency link power electronics interface for discrete power and data transfer," Doctoral dissertation, Department of Electrical Engineering, University of Illinois Chicago, 2011.
10. S. Mehrnami and S.K. Mazumder, "Discontinuous modulation scheme for a differential-mode Cuk inverter," IEEE Transactions on Power Electronics, vol. 30, no. 3, pp. 1242-1254, 2014.
11. S. K. Mazumder and K. Acharya, "Multiple Lyapunov function based reaching condition for orbital existence of switching power converters," in IEEE Transactions on Power Electronics, vol. 23, no. 3, pp. 1449-1471, May 2008, doi: 10.1109/TPEL.2008.921065.
12. D. Chatterjee and S. K. Mazumder, "Switching-sequence control of a higher order power-electronic system driving a pulsating load," in IEEE Transactions on Power Electronics, vol. 35, no. 1, pp. 1096-1110, Jan. 2020, doi: 10.1109/TPEL.2019.2915830.
13. Y. Qiu, M. Xu, K. Yao, J. Sun and F. C. Lee, "Multifrequency small-signal model for buck and multiphase buck converters," in IEEE Transactions on Power Electronics, vol. 21, no. 5, pp. 1185-1192, Sept. 2006, doi: 10.1109/TPEL.2006.880354.